Civil Engineering and Applied Solutions

Research Article

journal homepage: ceas.journals.umz.ac.ir

CEAS Civil Engineering and Applied Solutions

Finite Element Modeling of SMA-Confined Concrete: Influence of Winding Pitch and Temperature on Strength and Energy Dissipation

Moein Rezapour [a], Mehdi Ghassemieh [a*]

[a] *College of Engineering, School of Civil Engineering, University of Tehran, Tehran, Iran*

ARTICLE INFO

Keywords:
Shape memory alloy
Concrete confinement
Finite element modeling
Energy dissipation

Article history:
Received 14 September 2025
Accepted 11 October 2025
Available online 01 January 2026

ABSTRACT

This study presents a detailed finite element investigation of concrete cylinders confined with shape memory alloy (SMA) windings, focusing on the combined effects of winding pitch and temperature. The main objective is to evaluate how geometric configuration and thermal activation influence the compressive strength, ductility, and energy dissipation of confined concrete. The nonlinear response was modeled in ABAQUS using the Concrete Damaged Plasticity (CDP) framework for the concrete core and a user-defined FORTRAN subroutine to simulate the reversible austenite–martensite transformation of the SMA. The numerical model was validated against laboratory data, showing strong agreement between simulated and experimental stress–strain curves. Parametric analyses were performed for winding pitches of 5.3, 9, and 16 mm under temperatures of 30, 50, 70, and 90 °C. The results demonstrate that decreasing the winding pitch substantially enhances post-peak stability and energy absorption, while higher SMA temperatures improve confinement efficiency at large strains without significantly altering peak strength. The study confirms that tighter and thermally activated SMA windings provide more uniform stress distribution and superior energy dissipation. These findings highlight the potential of SMA-based active confinement as a reliable and adaptive strategy for seismic retrofitting and impact-resistant design of concrete structures.

1. Introduction

Ensuring the long-term durability and safety of concrete structures under lateral loads and variable environmental conditions has remained a central challenge in structural engineering. Enhancing the compressive strength and ductility of concrete is particularly critical in seismic and harsh exposure scenarios. Conventional confinement methods, such as steel hoops or fiber-reinforced polymers, have demonstrated reasonable effectiveness but exhibit notable limitations when subjected to temperature fluctuations and cyclic loading. Shape memory alloys (SMAs), owing to their unique properties including superelastic behavior, strain recovery, and mechanical stability over a wide temperature range, have emerged as a new generation of smart materials for concrete strengthening. Recent studies indicate that incorporating SMA wires or strips as active or passive wraps can substantially improve energy dissipation capacity and mitigate damage in concrete members. Nevertheless, the influence of key parameters, such as wrap pitch, temperature, and pre-tension level, on the overall response of SMA-confined concrete remains insufficiently clarified.

Enhancing the compressive capacity and ductility of concrete under axial and seismic loading remains a fundamental concern in structural engineering. Ordinary concrete, due to its inherent brittleness and limited post-peak strain capacity, is highly vulnerable to cyclic loading and large deformations. Traditional confinement techniques, such as steel stirrups and fiber-reinforced polymers (FRP), can improve strength and strain capacity, yet they exhibit notable shortcomings when exposed to temperature variations, cyclic fatigue, and progressive degradation of bond performance [1].

The advent of smart materials, particularly shape memory alloys (SMA), has opened new avenues for both active and passive

* Corresponding author.
E-mail addresses: m.ghassemieh@ut.ac.ir (M. Ghassemieh).

https://doi.org/10.22080/ceas.2025.30055.1042
ISSN: 3092-7749/© 2026 The Author(s). Published by University of Mazandaran.
This article is an open access article distributed under the terms and conditions of the Creative Commons Attribution (CC-BY) license (https://creativecommons.org/licenses/by/4.0/deed.en)
How to cite this article: Rezapour, M., Ghassemieh, M. Finite Element Modeling of SMA-Confined Concrete: Influence of Winding Pitch and Temperature on Strength and Energy Dissipation. Civil Engineering and Applied Solutions. 2026; 2(1): 33–45. doi:10.22080/ceas.2025.30055.1042.

strengthening of concrete members. Unique characteristics such as the shape-memory effect, superelastic behavior, high energy dissipation capacity, and the ability to induce intrinsic prestressing in SMA wires or strips have positioned these alloys as a promising alternative in structural engineering over the past two decades [2, 3]. Early reviews, including the seminal work by DesRoches et al. (2004), outlined the potential applications of SMA in seismic control and ductility enhancement while highlighting key research gaps that remain to be addressed [4].

The first experimental investigations focused on SMA-based confinement of concrete were conducted by Choi et al. By wrapping NiTi wires around concrete cylinders, they demonstrated marked improvements in compressive strength, ultimate strain, and energy dissipation compared with control specimens [5]. Subsequently, Shin and Andrawes introduced the concept of active confinement, wherein SMA wires, once heated and allowed to return to their original length, generate a stable confining pressure. Their findings indicated that this approach not only enhances strength but also promotes recentering and reduces residual deformation after unloading [6]. Building on this concept, Andrawes and et al. have conducted multiple studies validating the superior cyclic stability of SMA-confined columns relative to those reinforced with conventional transverse steel [7].

Gholampour and Ozbakkaloglu conducted a comprehensive study on both normal-strength and high-strength concrete, examining parameters such as SMA volumetric ratio and the austenitic/martensitic phase state [8, 9]. Their results showed that SMA confinement can increase compressive strength and ultimate strain by several multiples compared with control specimens, while producing a smoother stress–strain response that is highly favorable for seismic performance. Comparable findings have been reported in several other studies, including Park et al. who compared SMA wrapping with steel jacketing and observed a pronounced improvement in ductility [10].

The high cost of NiTi alloys and the manufacturing limits on wire diameter have, in recent years, shifted growing attention toward iron-based alloys (Fe-SMA). These materials retain the shape-memory effect and prestressing capability while being substantially more cost-effective and easier to install. Lee et al. in a laboratory investigation on circular reinforced-concrete columns under cyclic loading, reported significant gains in strength, ductility, and deformation stability through the application of Fe-SMA strips [11]. Similarly, Tran et al. demonstrated that using Fe-SMA wires in an active configuration markedly enhances the energy dissipation capacity of cylindrical specimens [12]. Recent studies combining Fe-SMA with FRP have further revealed a pronounced synergistic improvement in compressive capacity and post-peak softening behavior [13].

From a modeling perspective, the Concrete Damaged Plasticity (CDP) framework in ABAQUS has become the predominant approach for simulating the behavior of confined concrete. The model proposed by Lee and Fenves (1998) serves as the basis for many calibrations, providing robust capability to reproduce stress–strain curves in both compression and tension [14]. Seminal contributions by Martinez-Rueda and Elnashai and Dolce and Cardone (2001) formulated constitutive relationships for confined concrete and SMA under cyclic loading [15-17]. More recent numerical studies have advanced predictive stress–strain models for SMA-confined columns, offering valuable insights for the future of seismic design [18, 19].

Beyond full wrapping, SMA applications have also expanded into other domains such as beam–column connections, energy dissipation devices, and re-centering systems. Ocel et al. (2004) investigated beam–column joints equipped with SMA bolts and reported markedly higher re-centering capacity compared to conventional connections [20].

Despite the growing body of literature on SMA confinement, the combined effects of winding pitch and thermal activation remain insufficiently understood. This study therefore aims to quantify their influence on the strength, ductility, and energy dissipation of SMA-confined concrete through finite element simulations. Despite notable progress, future research must address issues such as behavior under eccentric loading, long-term durability, cyclic fatigue effects, and large-scale model calibration to establish the industrial viability of this technology. In the present study, numerical modeling in ABAQUS employing the Concrete Damaged Plasticity framework is used to examine the influence of wrap pitch and thermal conditions on the compressive strength and energy dissipation capacity of SMA-confined concrete specimens, aiming to advance the seismic and functional applications of this technology in concrete structures.

2. Shape memory alloys

Shape memory alloys (SMA) are a class of smart metallic materials capable of returning to their original configuration after experiencing substantial deformation. This unique behavior arises from a reversible phase transformation between two crystal structures: austenite and martensite (Fig. 1). Above the transformation temperature, the austenitic phase—characterized by a stable cubic lattice—exhibits high stiffness and elastic properties typical of conventional metals. Upon cooling or the application of stress, the crystal arrangement shifts to the martensitic phase, which has a monoclinic structure, is comparatively softer, and contains multiple variants that can easily reorient under stress, enabling large recoverable strains without permanent lattice slip [21]. The austenite-to-martensite transformation is shear-dominated and diffusionless; therefore, when the stimulus (heat or stress) is removed, the lattice promptly reverts to its original configuration.

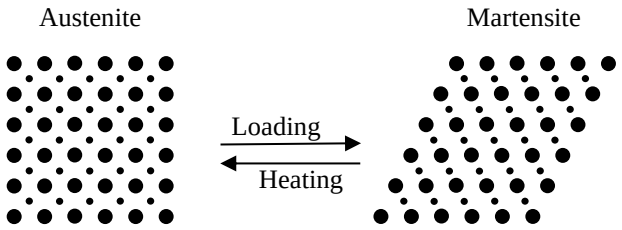

Fig. 1. Phase transformation of the SMA [19].

When an SMA deforms in the martensitic state, the apparent elongation results from the reorientation of martensitic variants rather than irreversible lattice changes. Reheating the alloy restores the austenitic structure, allowing complete shape recovery—commonly referred to as the shape memory effect. At temperatures above the austenite finish point, applied stress can induce stress-driven martensite, which reverts to austenite upon unloading, producing a closed stress–strain loop with significant hysteresis known as superelasticity [22, 23]. Chemical composition and heat treatment govern the transformation temperatures, enabling the design of alloys tailored to specific service environments. Together with their energy dissipation capacity and inherent re-centering capability, these characteristics make SMAs attractive for seismic retrofitting, active prestressing, and ductility enhancement of concrete members.

Prestressing in SMAs stems from the recovery strain during the martensite-to-austenite transformation. A wire or strip of SMA is first elongated or helically wound around a concrete member in the martensitic phase. Heating the material above its transformation temperature triggers the phase shift to austenite and induces a tendency to return to its pre-deformed length. Because the SMA is restrained by the surrounding concrete, this contraction manifests as a permanent circumferential compressive stress on the member, effectively providing an active confining pressure. This method eliminates the need for hydraulic jacks or mechanical anchors while ensuring a stable and uniform confinement from the onset of service. The resulting compressive hoop stress increases axial strength, delays crack initiation, and improves ductility and energy dissipation under cyclic loading. Consequently, SMA-based active prestressing offers an efficient strategy for enhancing the seismic performance of columns and other compression-dominated structural elements.

3. FEM modeling

In this study, the confinement behavior of concrete is modeled using the ABAQUS finite element software. Although ABAQUS provides a wide range of built-in material models—such as isotropic nonlinear behavior, concrete damaged plasticity, smeared crack approaches, Mohr–Coulomb and Drucker–Prager models for soils, and others—it does not natively include the constitutive behavior of shape memory alloys (SMAs). One of the advantages of ABAQUS, however, is its ability to incorporate user-defined material subroutines written in FORTRAN, allowing the introduction of new constitutive models. Therefore, the behavior of SMAs must first be coded in this environment and then linked to ABAQUS. Lagoudas, in his research at the University of Texas, developed such a subroutine for SMAs and performed the necessary verifications. Accordingly, in the present study, Lagoudas's user material subroutine is employed to model the SMA behavior [2].

The specimen modeled in this research was experimentally investigated by Hashemivand [24]. The concrete sample, with a compressive strength of 25 MPa and dimensions of 120 × 60 mm, was subjected to axial compression (Fig. 2). As shown in the figure, two steel rings, each 1 mm thick and 20 mm in height, were placed at the top and bottom of the specimen, and a 1-mm diameter Nitinol wire was wound around the specimen for ten turns.

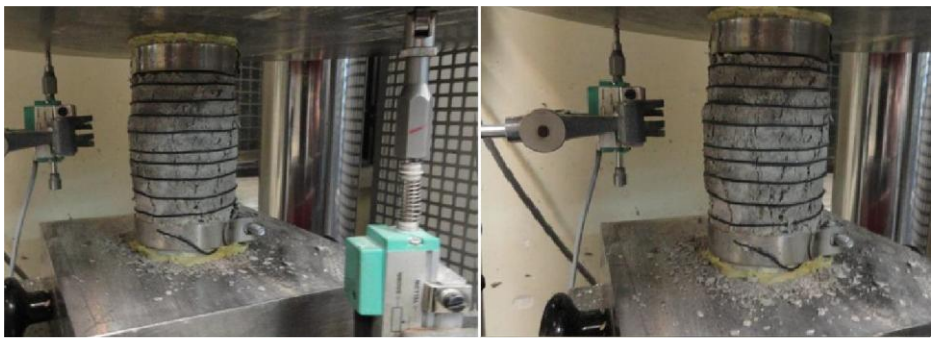

Fig. 2. Concrete specimen confined in the laboratory [24].

The nitinol tested in this study has mechanical properties as shown in Table 1. Numerical modeling of the behavior of concrete confined with a shape memory alloy was performed in the ABAQUS finite element environment to enable accurate simulation of the nonlinear response under axial loading. Concrete was defined using the Concrete Damaged Plasticity (CDP) model, which is among the most comprehensive approaches available for predicting compressive and tensile behavior as well as post-peak energy dissipation. This model accounts for strain softening, modulus degradation, and the gradual reduction of load-carrying capacity due to microcracking, and it has been widely applied for analyzing the quasi-brittle response of concrete in both compression and tension.

Table 1. Mechanical properties of the shape memory alloy at 30 °C.

Elastic modulus	7.5×10^4 MPa
Start stress for austenite-to-martensite transformation	385 MPa
Finish stress for austenite-to-martensite transformation	516 MPa
Start stress for martensite-to-austenite transformation	356 MPa
Finish stress for martensite-to-austenite transformation	202 MPa
Superelastic strain range	6.25 %
Density	65 kN/m³

Key parameters, including the internal friction angle, dilation ratio, initial elastic modulus, hardening coefficients, and damage factors, were determined according to the software guidelines and available experimental data. The compressive stress–strain curve was calibrated based on the cylindrical compressive strength and empirical coefficients; in the pre-peak region, the response was assumed to be nearly linear, while beyond the peak an exponential softening function was adopted to reproduce the gradual strength decay. In tension, a progressive damage law governed by fracture energy was implemented to realistically capture the transition from elastic behavior to microcracking and failure. This framework enabled prediction of modulus reduction and stiffness degradation due to cumulative damage, and the load–strain curves obtained from the model showed good agreement with trends reported in experimental studies.

In the concrete damaged plasticity (CDP) model implemented in ABAQUS, two key parameters are defined to represent the degradation of material capacity: dc (damage in compression) and dt (damage in tension). These coefficients describe the fraction of effective stiffness lost due to microcracking and softening, varying from zero (undamaged) to one (fully damaged).

Under compression, once strain exceeds the peak point, progressive microcracking and particle crushing reduce the effective modulus. This process is represented by the dc–εc curve, where dc begins to increase after the peak strain, producing a linear or exponential reduction in concrete stiffness. The curve shape is typically calibrated against the compressive fracture energy (Gc) and uniaxial test results to ensure that the area under the curve matches the dissipated energy. In tension, concrete exhibits predominantly brittle behavior accompanied by crack opening. Beyond the peak tensile stress, a rapid loss of capacity occurs, and softening is captured through the dt parameter. The dt–εt relationship is commonly specified as linear or exponential so that the area under the tensile stress–strain curve corresponds to the tensile fracture energy (Gt). During the analysis, ABAQUS computes the effective stiffness of each element as (1−d).E, where d represents dc or dt depending on the loading mode. This mechanism allows the model to reproduce both strength degradation and modulus reduction during cyclic or post-peak loading (Fig. 3).

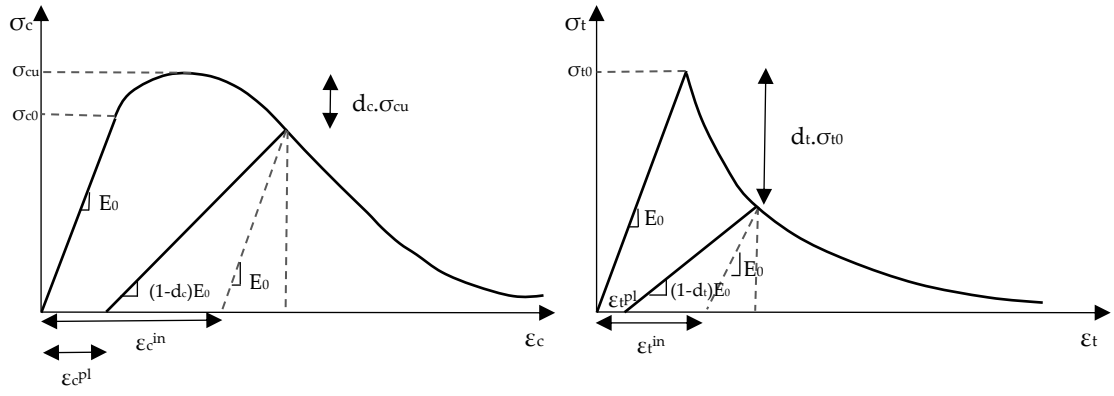

(a) **(b)**

Fig. 3. Dependence σ-ε for CDP model (a) in compression (b) in tension.

By accurately defining the dc and dt curves based on experimental data, numerical simulations can realistically represent microcrack initiation, gradual stiffness loss, and energy absorption capacity of concrete under both compression and tension, enabling reliable prediction of the nonlinear response of SMA-confined members. Since the loading in this study is predominantly monotonic, these two parameters were adopted accordingly.

The behavior of the shape memory alloy (SMA) was implemented through a user-defined subroutine (FORTRAN code) to reproduce the reversible austenite–martensite transformation and the associated mechanical hysteresis in the software. Within this code, transformation temperatures elastic moduli of the two phases, maximum recoverable strain, and temperature-dependent stress–strain curves were specified as input parameters. Stress-induced transformation and the shape-memory effect were formulated using thermodynamically based lattice-shear equations within an iterative algorithm to capture the pseudoelastic response and energy dissipation due to the hysteresis loop.

To simulate active prestressing, the initial length of the SMA element was modified in the martensitic state, and during a thermal analysis step the temperature was raised above Af, triggering length recovery and inducing circumferential compressive stress in the concrete member. This approach enables incorporation of both nonlinear behavior and the intrinsic prestressing effect of the SMA under axial loading, producing results consistent with experimental trends.

For accurate transfer of confining stress, the interaction between the SMA winding and the outer concrete surface was modeled as surface-to-surface contact: normal behavior was defined as hard contact, while a tangential friction coefficient of 0.3 was assigned to allow limited but realistic slip between wire and concrete. This formulation ensures that the compressive stress generated by SMA recovery is fully transmitted to the concrete wall, providing a realistic representation of active confinement. The interfaces between concrete and the loading platens were modeled using a tie constraint to apply uniform axial stress.

As observed in the experimental model, the concrete specimen consists of three main components: the concrete core, the steel restraining rings, and the winding. These components were modeled in the ABAQUS finite element environment as illustrated in Fig. 4. According to these figures, the elements used for the concrete core and the winding are eight-node solid brick elements (C3D8), while for ease of computation, the restraining rings were modeled using four-node shell elements (S4).

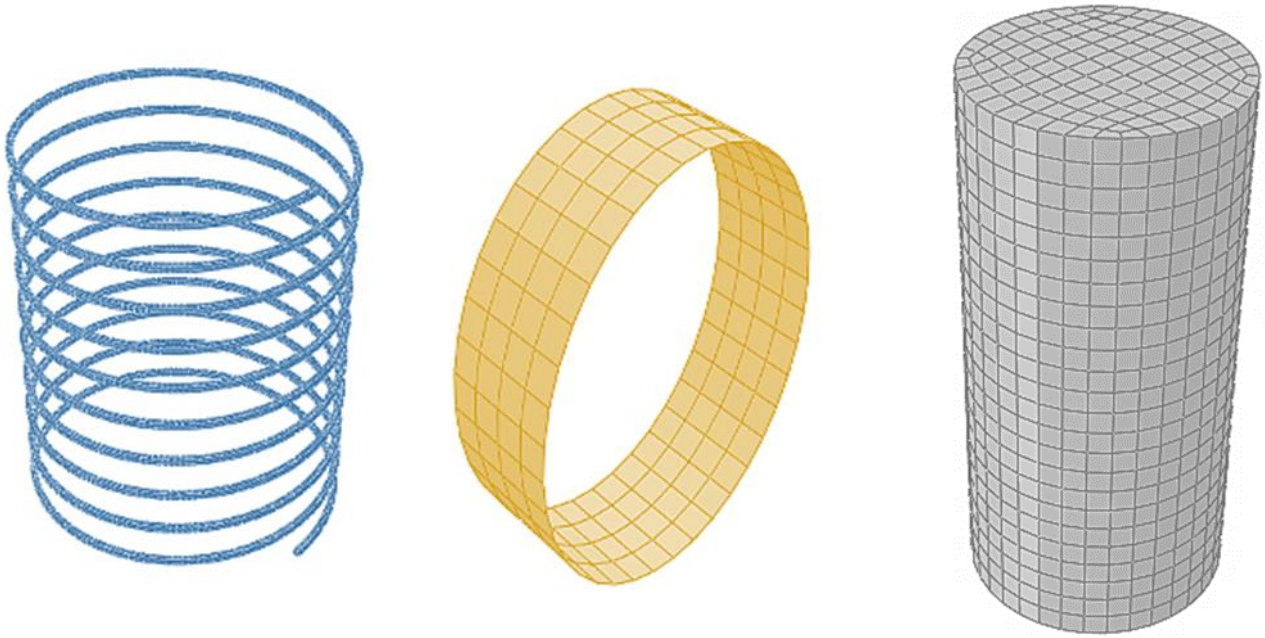

Fig. 4. Meshing of the concrete core, steel restraining rings, and shape memory alloy winding.

To connect these components, a tie interaction was defined. This interaction constrains the connected parts as if they were bonded, preventing any relative displacement between corresponding nodes. Fig. 5. Final finite element model and deformed shape, showing correct performance of the defined interactions.

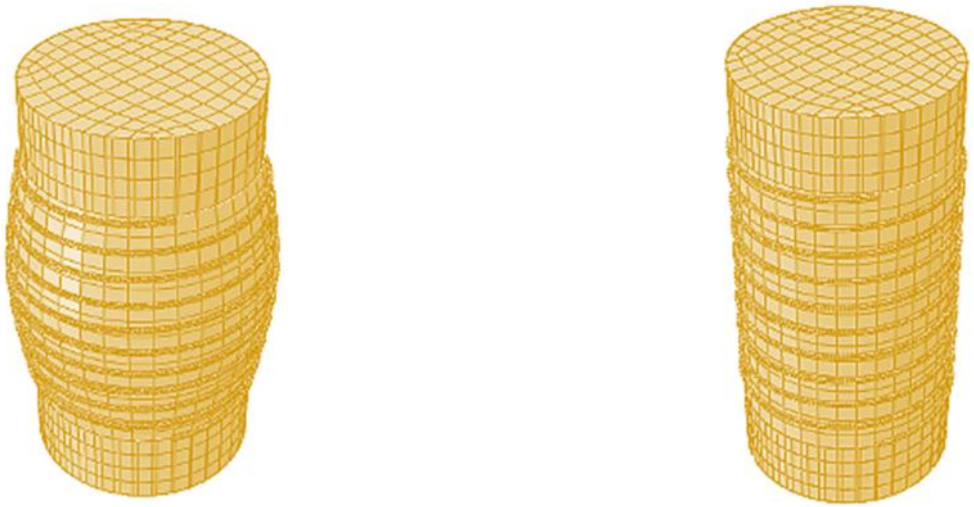

Fig. 5. Final finite element model and deformed configuration.

Fig. 6. Comparison of stress–strain curves for the experimental and numerical models. The figure demonstrates that the numerical model closely captures the nonlinear behavior observed in the laboratory specimen, including both the pre-peak stiffness and post-peak softening, validating the accuracy of the finite element modeling approach.

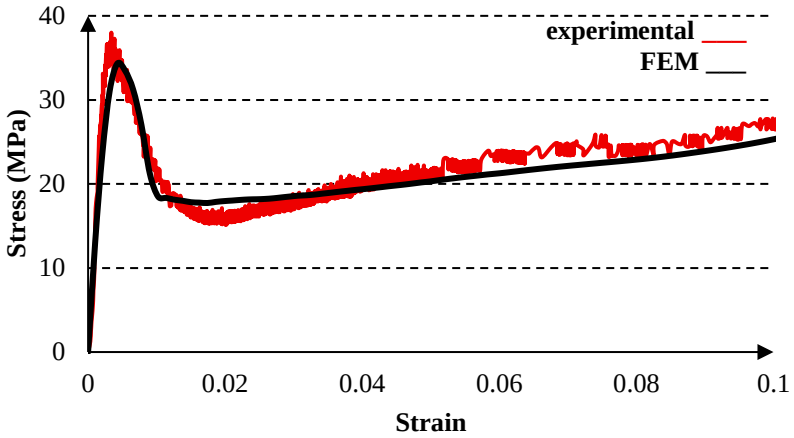

Fig. 6. Validation between experimental and numerical models.

What has been presented so far as the basis of the study primarily consisted of explanations regarding concrete confinement and its behavior under both active and passive conditions. In Chapter 4, the methodology for modeling confinement in ABAQUS was described, and a laboratory specimen was used to validate the numerical approach. In this chapter, to investigate more precisely the effect of shape memory alloys on the confinement of concrete, various configurations of the smart winding at different temperatures are examined. To evaluate these behaviors, several parameters including strength, energy dissipation, and others are considered.

4. Results

4.1. Effect of Winding Pitch

The winding pitch, defined as the center-to-center distance between adjacent turns, determines the effective number of SMA windings per specimen height. The first parameter investigated in this study is the winding pitch in concrete confinement (here, the pitch refers to the center-to-center distance of one complete turn). To examine this effect, three models with different pitches (16 mm, 9 mm, and 5.3 mm) were considered, with confinement provided by Nitinol wires (Fig. 7).

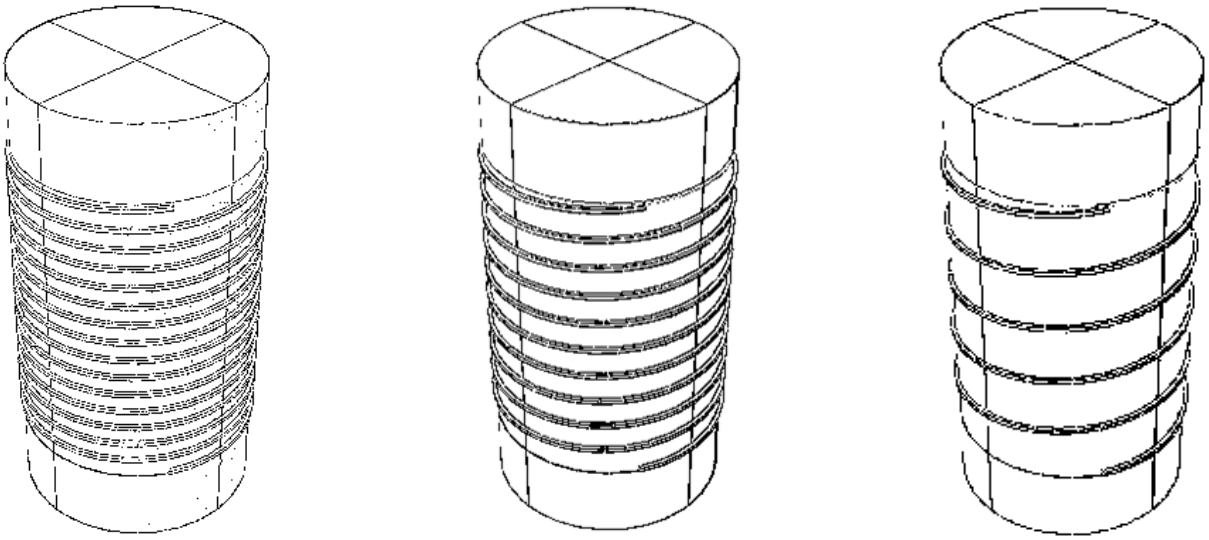

(a) **(b)** **(c)**

Fig. 7. Models with different winding pitches: (a) 5.3 mm pitch, (b) 9 mm pitch, (c) 16 mm pitch.

The models shown in Fig. 7 were subjected to axial compression applied from the top. This loading was applied until the specimens failed, causing significant lateral expansion in the concrete cores. With this expansion, the surrounding shape memory alloy (SMA) windings become active, inducing confinement in the specimen.

To investigate the effect of the number of SMA windings on the overall confinement of the system, the three specimens were analyzed under compressive loading. Fig. 8 presents the stress–strain curves for these systems at 30 °C. As expected, increasing the winding density enhances the strength of the specimens. Moreover, because SMAs exhibit strain-hardening behavior at large deformations, higher winding density leads to greater confinement capacity at elevated strains. While an increased number of windings slightly raises the peak compressive strength, its effect becomes more pronounced in the post-peak, large-strain region.

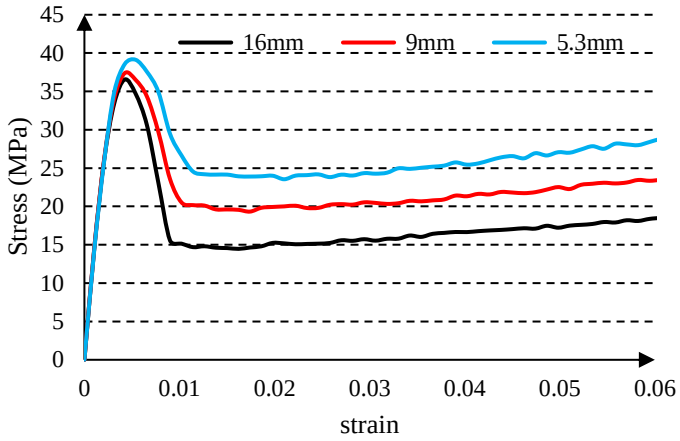

Fig. 8. Compressive stress–strain curves of specimens with different winding densities at 30 °C.

As illustrated in Fig. 8, reducing the winding pitch significantly increases the energy dissipation capacity of the concrete specimens. This effect occurs because closer windings engage the shape memory alloy more effectively during lateral expansion, providing stronger confinement and enhanced post-peak performance. At 30 °C, the total energy dissipated by the specimens with winding pitches of 16 mm, 9 mm, and 5.3 mm is 699 J, 902 J, and 1091 J, respectively, demonstrating a clear trend of improved energy absorption with increasing winding density. This indicates that optimizing the winding configuration can play a crucial role in enhancing both strength and ductility of SMA-confined concrete members.

Fig. 9 illustrates the distribution of von Mises stress within the components and at different cross-sections of the concrete specimens. These images correspond to the moment when the longitudinal strain of the concrete specimens reaches 0.12. Focusing on the stress distribution within the concrete core, it is evident that the winding pitch significantly influences the stress profile. As shown, specimens with shorter winding pitches, or, in other words, more closely spaced windings, can sustain higher stresses at elevated strains. For instance, at a longitudinal strain of 0.12, the maximum stress in the concrete cores for specimens with winding pitches of 16 mm, 9 mm, and 5.3 mm is 37.3, 48.4, and 59.1 MPa, respectively.

Examining a cross-section of the concrete core reveals that the stress near the top and bottom circumferences is close to zero. Similarly, stress near the mid-height of the concrete core is approximately zero. As noted, the primary parameter responsible for these variations in stress distribution is the configuration of the SMA winding. The stress distribution within the windings themselves also varies. Because the mid-height of the concrete cylinder experiences the largest radial strain, the corresponding strain in the SMA is greatest there. However, when the winding pitch is short, i.e., the windings are densely arranged, the radial strain is reduced. Consequently, in specimens with a 5.3 mm winding pitch, both the radial strain and the induced stress in the SMA are lower compared to the other models.

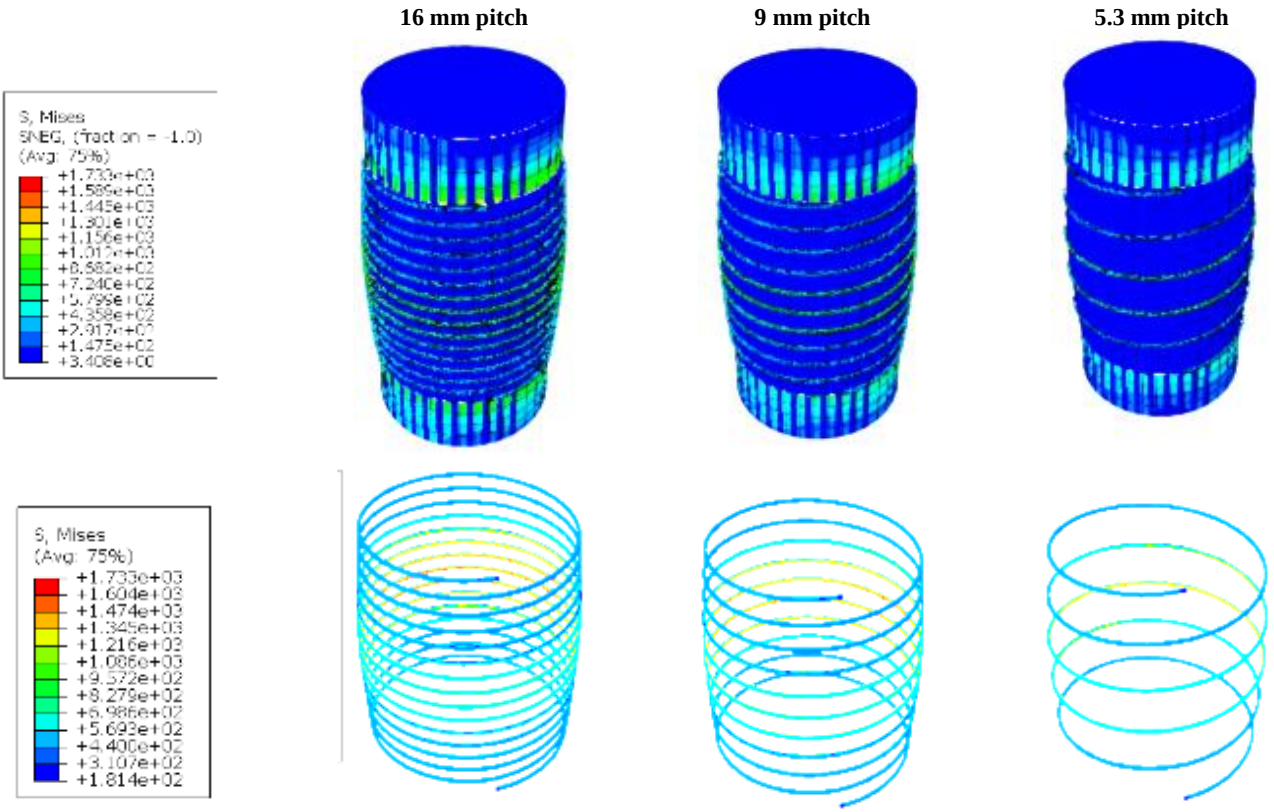

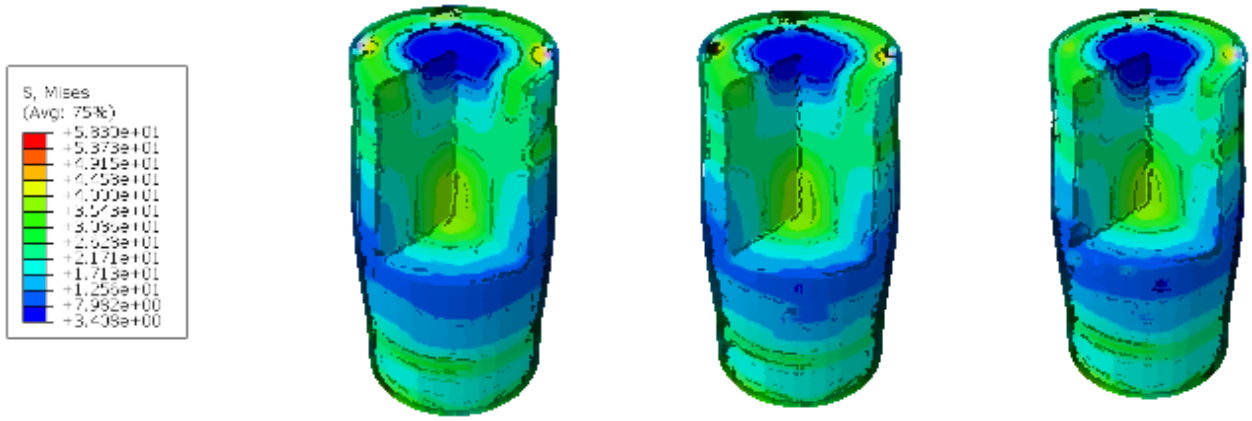

Fig. 9. Concrete specimens with winding pitches of 5.3 mm, 9 mm, and 16 mm at 30 °C.

4.1. Effect of temperature

The behavior of shape memory alloys (SMAs) is directly dependent on temperature. Upon heating, these alloys transform into the austenite phase, which increases their confinement capacity. The models studied in this research involve SMAs with an activation temperature of 30 °C. According to the numerical stress–temperature behavior of the SMAs, the phase transformation is dependent on both stress and temperature.

To investigate the effect of SMA temperature on the winding and overall confinement, in addition to 30 °C, the models were also analyzed at 50 °C, 70 °C, and 90 °C. At these elevated temperatures, the confinement capacity of the SMAs is increased. Fig. 10 illustrates the effect of temperature on confinement for models with winding pitches of 16 mm, 9 mm, and 5.3 mm. As shown, higher SMA temperatures result in greater strength of the concrete specimens at large deformations. On the other hand, the peak compressive strength of the specimens is only minimally affected by temperature, indicating that the peak strength primarily depends on the winding configuration and pitch.

An important observation regarding SMA confinement is that it significantly enhances the concrete's capacity at high strains. Consistent with the results, the stronger the confinement, the greater the increase in strength at elevated strains. This trend can substantially improve the energy absorption capacity of the specimens.

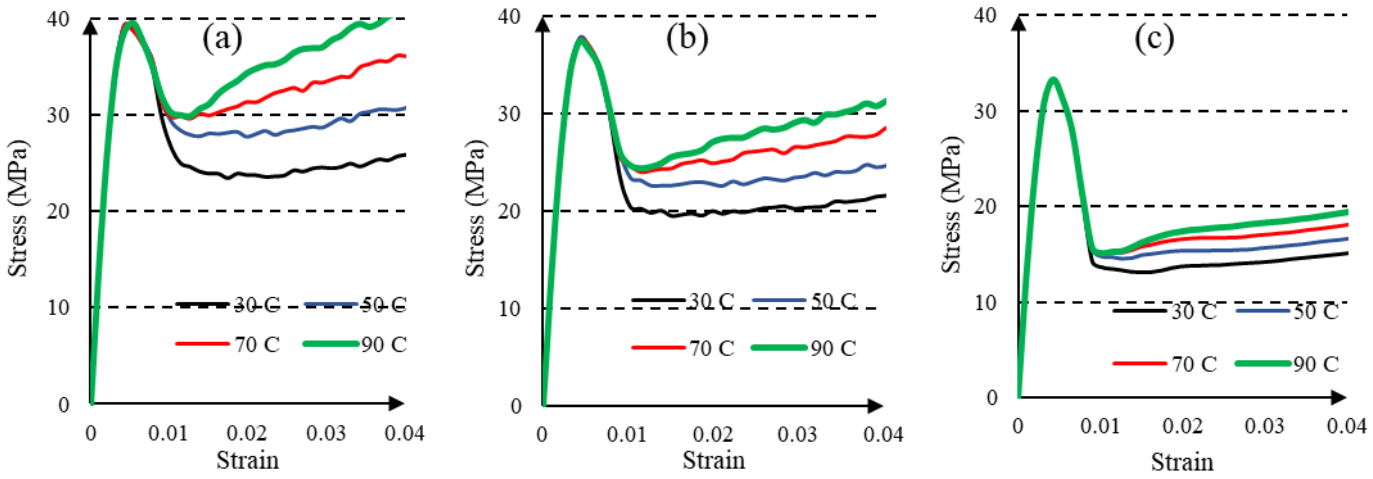

Fig. 10. Compressive stress–strain curves of SMA-confined concrete specimens with winding pitches of (a) 5.3 mm, (b) 9 mm, and (c) 16 mm at different temperatures.

According to Table 2, the energy dissipation capacities of the specimens at different temperatures are presented. Comparison of these data indicates that, as the temperature of the shape memory alloy (SMA) increases, the system's ability to absorb and dissipate energy grows in an approximately linear manner. The corresponding plots for all three concrete models exhibit an upward trend, reflecting the more effective activation of the confining wraps at higher temperatures.

It is noteworthy that the slope of energy growth is not identical across specimens; the degree of wrapping density has a direct influence on this slope. The denser the winding, the greater the rate of increase in energy dissipation with temperature. Specifically, the slopes for specimens with winding pitches of 5.3, 9, and 16 mm are approximately 7.97, 5.46, and 2.85, respectively. This demonstrates that specimens containing a larger volume of SMA exhibit higher sensitivity to temperature changes and greater energy absorption capacity. Such behavior underscores the importance of selecting an appropriate winding pitch when designing systems intended to withstand cyclic and impact loading.

Table 2. Energy absorbed at different temperatures and steps.

winding pitches	30ºC	50ºC	70ºC	90ºC
5.3 mm	1120 J	1272 J	1425 J	1578 J
9 mm	923 J	1025 J	1135 J	1240 J
16 mm	720 J	781 J	828 J	883 J

In Figs. 11 to 13, the stress distribution for specimens with a 16 mm winding pitch at different temperatures is illustrated. These plots clearly indicate that at higher temperatures, the confined concrete specimens sustain greater stress. For instance, at a longitudinal strain of 0.12, the maximum stress reaches about 43 MPa at 90 °C, compared with roughly 37 MPa at 30 °C. From the presented figures, it can be inferred that elevated temperature exerts a direct influence on the stress distribution within the confined concrete, with the most pronounced effects observed in the concrete core itself. As the SMA strength rises with temperature, the lateral expansion of the concrete is reduced. Limiting lateral dilation is critical for confinement effectiveness because uncontrolled expansion accelerates loss of strength and crushing. Consequently, in specimens where the SMA temperature is higher, the alloy delays premature dilation, allowing the core to carry greater stress, as clearly reflected in the figures.

Another notable point is that, in specimens with lower SMA temperatures, the stress at the mid-height of the concrete tends to drop toward zero. This indicates increased local crushing in that region, primarily due to greater lateral strain. As the SMA temperature increases and restrains dilation, stress at mid-height remains farther from zero, signifying improved confinement. Moreover, in models where the winding pitch is tighter, the stress in the core is less prone to drop toward zero, since a greater SMA volume contributes to enhanced thermal sensitivity. For example, in a specimen with a 5.3 mm pitch at 90 °C, the mid-core stress almost never approaches zero.

Stress distribution within the SMA itself also varies. Across all specimens, the SMA segments located near the mid-height experience the highest strain and stress, while those near the top and bottom surfaces are subjected to almost negligible stress. Overall, specimens with denser windings exhibit lower SMA stress under identical strain levels because the load is shared among more wraps. However, with increasing temperature, the trend shifts: specimens at 90 °C display higher stress in the SMA. This is because the elevated temperature enhances the alloy's stiffness; for two identical SMA elements subjected to the same strain, the one at a higher temperature develops greater stress. Since the applied loading is displacement-controlled, all specimens undergo the same axial strain, and radial strain differences remain minor. Consequently, under higher temperatures, the SMA exhibits higher stress, even though radial expansion is slightly reduced, reflecting the thermally enhanced mechanical response.

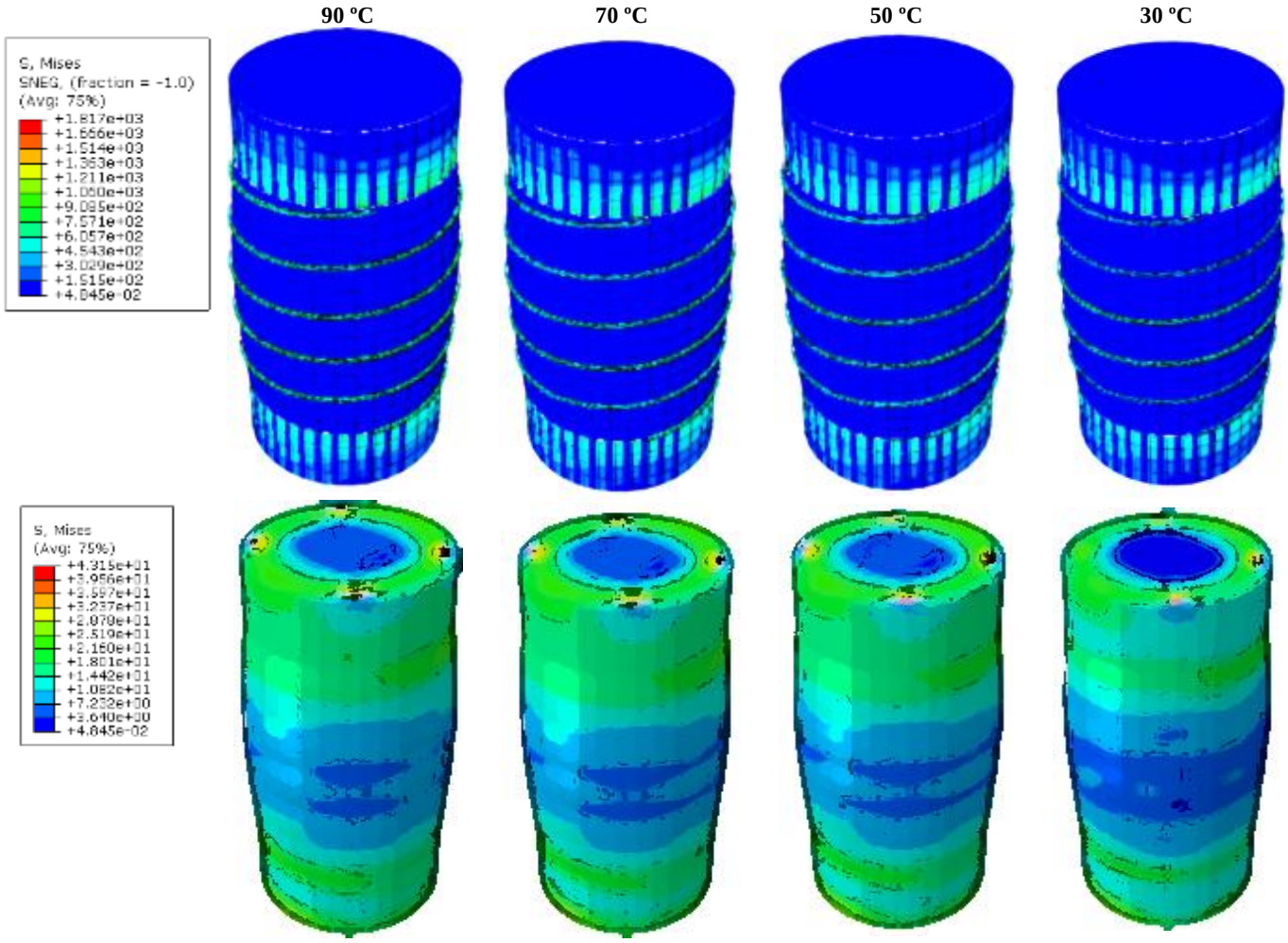

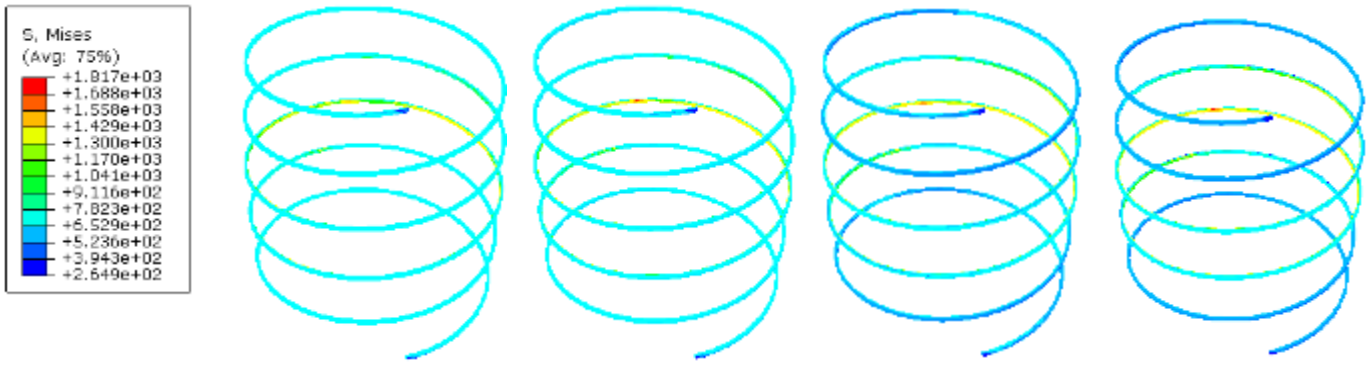

Fig. 11. 16 mm pitch concrete specimens at different temperatures

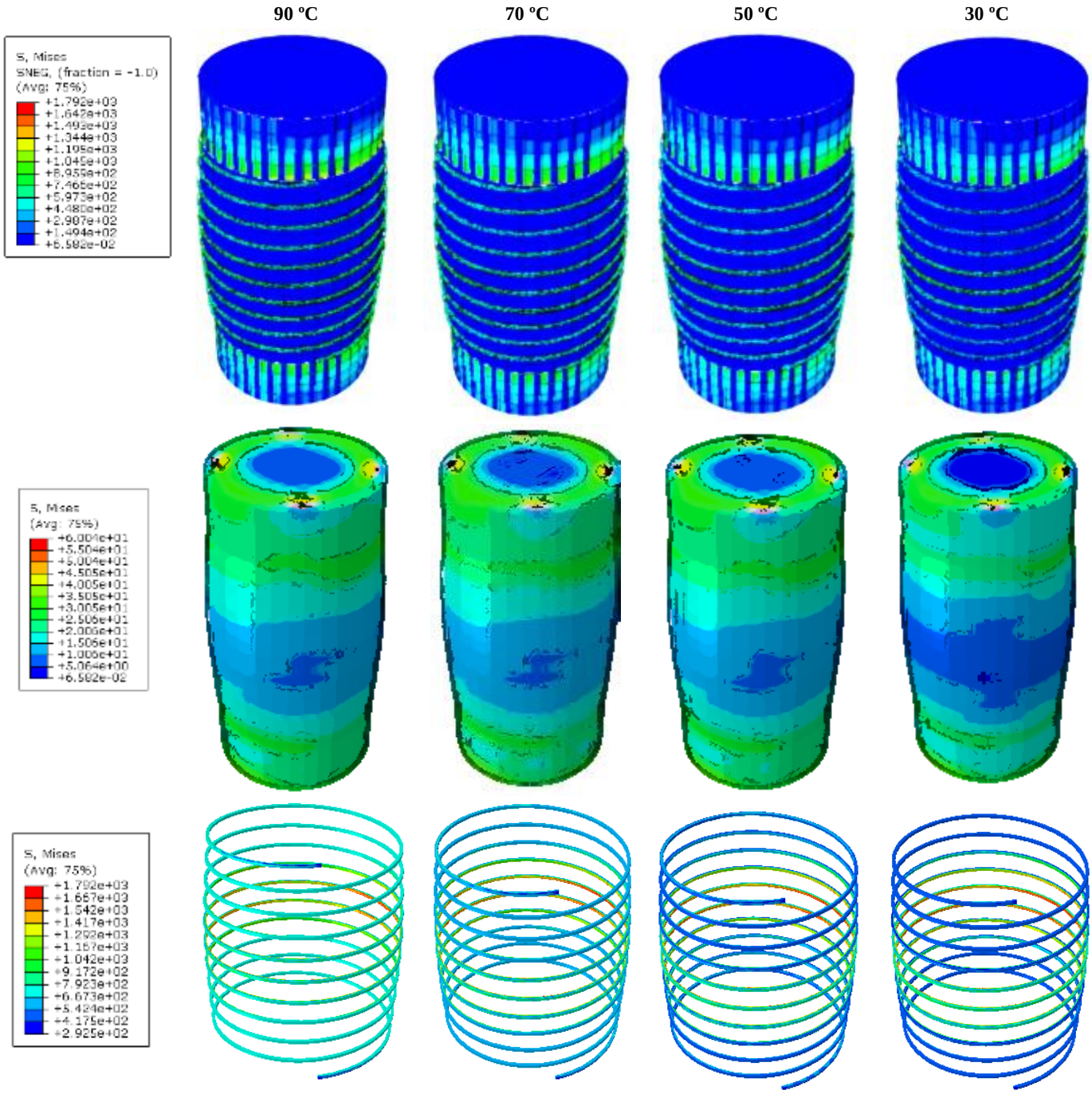

Fig. 12. 9 mm pitch concrete specimens at different temperatures.

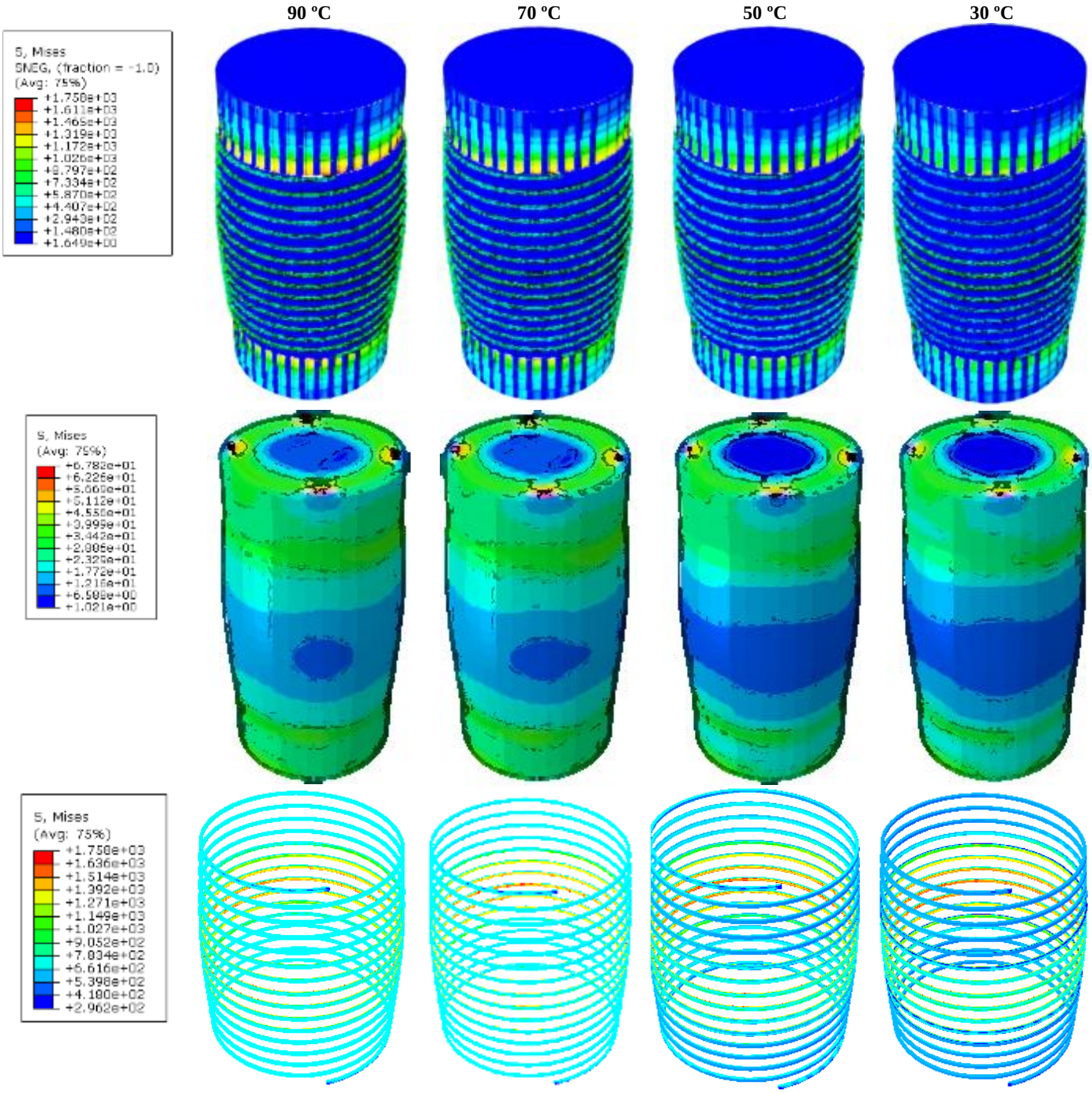

Fig. 13. 5.3 mm pitch concrete specimens at different temperatures.

5. Conclusion

This study numerically investigated the axial behavior of concrete specimens confined with shape memory alloy (SMA) windings using the Concrete Damaged Plasticity (CDP) model in ABAQUS. The main findings are summarized as follows:

1. Model validation:

The proposed FE model, incorporating a user-defined SMA subroutine, accurately reproduced the experimental stress–strain response, including pre-peak stiffness, peak strength, and gradual post-peak softening.

2. Effect of winding pitch:

Decreasing the winding pitch (increasing SMA density) significantly enhanced both the axial strength and the energy dissipation capacity of the confined concrete. At 30 °C, specimens with pitches of 5.3, 9, and 16 mm dissipated 1091 J, 902 J, and 699 J, respectively.

3. Effect of temperature:

Increasing the SMA temperature improved confinement effectiveness at large strains while exerting minimal influence on the peak strength. Elevated temperatures delayed lateral dilation, resulting in higher stress retention and ductility.

4. Stress distribution:

Stress field analysis revealed that denser windings produced more uniform stress profiles across the concrete core and minimized mid-height stress loss, indicating improved confinement uniformity.

5. Thermal sensitivity:

The slope of energy growth with temperature depended on winding density; specimens with greater SMA volume exhibited steeper increases in dissipated energy, confirming the strong thermal responsiveness of tight windings.

6. Practical implications:

SMA-based confinement provides a self-stabilizing and temperature-responsive confinement mechanism that can markedly improve seismic resilience and impact resistance in concrete members.

Future research should address cyclic and fatigue loading, durability under environmental exposure, and scaling effects for large structural elements. Further validation using hybrid SMA–FRP confinement and full-scale column testing is also recommended.

Statements & Declarations

Author contributions

Moein Rezapour: Investigation, Formal analysis, Validation, Resources, Writing - Original Draft, Writing - Review & Editing.

Mehdi Ghassemieh: Conceptualization, Methodology, Project administration, Supervision, Writing - Review & Editing.

Funding

The authors received no financial support for the research, authorship, and/or publication of this article.

Data availability

The data presented in this study will be available on interested request from the corresponding author.

Declarations

The authors declare no conflict of interest.

References

[1] Song, G., Ma, N., Li, H.-N. Applications of shape memory alloys in civil structures. Engineering structures, 2006; 28: 1266-1274. doi:10.1016/j.engstruct.2005.12.010.

[2] Lagoudas, D. C. Shape Memory Alloys. 1st ed. New York (NY): Springer New York; 2008. doi:10.1007/978-0-387-47685-8.

[3] Yamauchi, K., Ohkata, I., Tsuchiya, K., Miyazaki, S. Shape Memory and Superelastic Alloys: Applications and Technologies. 1st ed. Amsterdam (NL): Elsevier; 2011. doi:10.1533/9780857092625.

[4] Rashed, G. Seismic vibration control of frame structure using shape memory alloy, (PhD Thesis). Dhaka (BD): Bangladesh University of Engineering and Technology; 2013.

[5] Choi, E., Nam, T.-h., Cho, S.-C., Chung, Y.-S., Park, T. The behavior of concrete cylinders confined by shape memory alloy wires. Smart Materials and Structures, 2008; 17: 065032. doi:10.1088/0964-1726/17/6/065032.

[6] Shin, M., Andrawes, B. Lateral Cyclic Behavior of Reinforced Concrete Columns Retrofitted with Shape Memory Spirals and FRP Wraps. Journal of Structural Engineering, 2011; 137: 1282-1290. doi:10.1061/(ASCE)ST.1943-541X.0000364.

[7] Andrawes, B., Shin, M., Wierschem, N. Active Confinement of Reinforced Concrete Bridge Columns Using Shape Memory Alloys. Journal of Bridge Engineering, 2010; 15: 81-89. doi:10.1061/(ASCE)BE.1943-5592.000003.

[8] Gholampour, A., Ozbakkaloglu, T. Shape memory alloy (SMA)-confined normal-and high-strength concrete. In: 20th International Conference on Composite Structures: proceedings; 2017; Bologna, Italy. p. 114.

[9] Gholampour, A., Ozbakkaloglu, T. Understanding the compressive behavior of shape memory alloy (SMA)-confined normal-and high-strength concrete. Composite Structures, 2018; 202: 943-953. doi:10.1016/j.compstruct.2018.05.008.

[10] Park, J., Choi, E., Park, K., Kim, H.-T. Comparing the cyclic behavior of concrete cylinders confined by shape memory alloy wireor steel jackets. Smart Materials and Structures, 2011; 20: 094008. doi:10.1088/0964-1726/20/9/094008.

[11] Lee, T., Jeong, S., Woo, U., Choi, H., Jung, D. Experimental Evaluation of Shape Memory Alloy Retrofitting Effect for Circular Concrete Column Using Ultrasonic Pulse Velocity. International Journal of Concrete Structures and Materials, 2023; 17: 13. doi:10.1186/s40069-022-00574-0.

[12] Tran, H., Balandraud, X., Destrebecq, J. Improvement of the mechanical performances of concrete cylinders confined actively or passively by means of SMA wires. Archives of Civil and Mechanical Engineering, 2015; 15: 292-299. doi:10.1016/j.acme.2014.04.009.

[13] Miłek, T. Experimental Determination of Material Boundary Conditions for Computer Simulation of Sheet Metal Deep Drawing Processes. Advances in Science and Technology. Research Journal, 2023; 17: 360-373. doi:10.12913/22998624/172364.

[14] Lee, J., Fenves, G. L. Plastic-Damage Model for Cyclic Loading of Concrete Structures. Journal of engineering mechanics, 1998; 124: 892-900. doi:10.1061/(ASCE)0733-9399(1998)124:8(892.

[15] Martínez-Rueda, J. E., Elnashai, A. S. Confined concrete model under cyclic load. Materials and structures, 1997; 30: 139-147. doi:10.1007/BF02486385.

[16] Dolce, M., Cardone, D. Mechanical behaviour of shape memory alloys for seismic applications 2. Austenite NiTi wires subjected to tension. International journal of mechanical sciences, 2001; 43: 2657-2677. doi:10.1016/S0020-7403(01)00050-9.

[17] Dolce, M., Cardone, D. Mechanical behaviour of shape memory alloys for seismic applications 1. Martensite and austenite NiTi bars subjected to torsion. International journal of mechanical sciences, 2001; 43: 2631-2656. doi:10.1016/S0020-7403(01)00049-2.

[18] Rezapour, M., Ghassemieh, M., Motavalli, M., Shahverdi, M. Numerical Modeling of Unreinforced Masonry Walls Strengthened with Fe-Based Shape Memory Alloy Strips. Materials, 2021; 14: 2961. doi:10.3390/ma14112961.

[19] Ghassemieh, M., Rezapour, M., Sadeghi, V. Effectiveness of the shape memory alloy reinforcement in concrete coupled shear walls. Journal of Intelligent Material Systems and Structures, 2017; 28: 640-652. doi:10.1177/1045389X16657200.

[20] Ocel, J., DesRoches, R., Leon, R. T., Hess, W. G., Krumme, R., Hayes, J. R., Sweeney, S. Steel Beam-Column Connections Using Shape Memory Alloys. Journal of Structural Engineering, 2004; 130: 732-740. doi:10.1061/(ASCE)0733-9445(2004)130:5(73).

[21] Rezapour, M., Ghassemieh, M. Numerical Investigation of Fe-SMA Strengthened Masonry Walls under Lateral Loading. Civil Engineering and Applied Solutions, 2025; 1: 1-15. doi:10.22080/ceas.2025.29594.1022.

[22] Rezapour, M., Ghassemieh, M. Investigating the influence of superelastic dampers on the behavior of double-sided knee braces. Journal of Steel & Structure, 2024; 18: 69-85.

[23] Banihashem, S. M., Rezapour, M., Attarnejad, R., Sanei, M. Evaluating the Effectiveness of a New Self-Centering Damper on a Knee Braced Frame. Shock and Vibration, 2023; 2023: 6335011. doi:10.1155/2023/6335011.

[24] Hashemvand, A. Investigation of Composite Compressive Properties of Concrete Confined with Shape Memory Alloys, (PhD Thesis). Tehran (IR): Tehran university; 2015.